Polarization-dependent perfect absorbers/reflectors based on a three-dimensional metamaterial

Xiang Xiong, Zhen-Hong Xue, Cong Meng, Shang-Chi Jiang, Yu-Hui Hu, Ru-Wen Peng, and Mu Wang*
National Laboratory of Solid State Microstructures and Department of Physics, Nanjing University, Nanjing 210093, China
(Received 19 May 2013; revised manuscript received 30 July 2013; published 3 September 2013)

Conventionally a flat, shiny metal surface can be used as a reflector. Here we show that a microstructured metal surface can be switched from a perfect reflector to a perfect absorber by merely changing the polarization of the incident light. The structure consists of arrays of three-dimensional standing U-shaped resonators (SUSRs), which are fabricated by two-photon polymerization followed by blanket coating of the metal. For the incidence with a specific polarization, light can be perfectly reflected. By changing the polarization of incident light for 90°, light neither transmits nor reflects. Since the electromagnetic resonance occurs in between the standing arms of a U-shaped resonator, the heat generated in the absorption process is expected to dissipate more easily. The thermal stability of the SUSR absorber has also been investigated.

DOI: 10.1103/PhysRevB.88.115105 PACS number(s): 78.68.+m, 78.20.Ci, 42.25.Ja, 42.25.Bs

I. INTRODUCTION

It has been known for thousands of years that a flat metal surface can be used as a mirror.[1] In fact, a metal film merely a few tens of nanometers in thickness may reflect more than 99% of the light over a broad band of frequency.[2] An absorber, however, possesses the opposite property. It neither reflects nor transmits the incident light. Designing, fabrication, and characterization of metamaterial absorbers have attracted much attention recently due to the requirements in research of photovoltaic solar cells,[3] microbolometers,[4] spatial imaging,[5] thermal emission control,[6] and highly sensitive detectors.[7,8] With elaborately designed metastructures, different kinds of absorbers have been achieved at different resonant frequencies. By introducing anisotropy in the building blocks, polarization-sensitive[9–15] absorbers are realized, where only the incident light with specific polarization may excite the resonance in the strucure. Due to the resonance feature, a conventional absorber usually works at a very narrow frequency band. By designing structures with multiresonance frequencies, it is possible to realize a broadband absorber.[16–20] Up to now, most metamaterial absorber fabrication follows the idea of building sandwiched multilayers, where the top layer is a patterned metallic structure separated from the bottom metallic film by a dielectric interlayer.[10,20–23] In such a multilayer sandwich design, despite the fact that the metal itself is thermally conductive, the dielectric layer accommodates electromagnetic resonance, and the heat generated therein cannot be dissipated efficiently. The heat accumulation may lead to surface melting and reshaping of the structure,[24,25] and eventually damage the absorber. In contrast to previous multilayer sandwich designs, recently a polarization-sensitive absorber with metallic grooves has been theoretically proposed.[9] With conventional microfabrication techniques, however, it remains challenging to fabricate these structures over a large area.

In this article we demonstrate a three-dimensional (3D) polarization-sensitive structure made of standing U-shaped resonators (SUSRs). With this structure, we are able to switch a perfect reflector to a perfect absorber by merely tuning the polarization of the incident light. For the incidence with a specific polarization, the light reflects perfectly from the surface. By changing the polarization of incident light to the perpendicular orientation, however, the incident light neither transmits nor reflects from the surface. This feature makes the SUSRs very useful in manipulating polarization of light and detecting electromagnetic waves with specific polarization. It is noteworthy that for SUSRs, resonance occurs in the free space between the standing tines of the U-shaped metal structure, so the generated heat in absorption is expected to be dissipated more easily.

II. STRUCTURAL DESIGN

The building block of the SUSRs is constructed as follows. An array of U-shaped resonators is fabricated on the glass substrate by two-photon polymerization of UV-curable negative photoresist. Then a continuous metallic thin film covers the surface of the substrate and the SUSR units. A sketch of the SUSR unit is shown in Fig. 1(a). The opening of the SUSR points upward to the z direction. The unit in Fig. 1(a) is repeated along the x and y directions with lattice constant L_x and L_y, respectively. The normal incident light propagates in the $-z$ direction and the polarization angle is θ. The software based on the finite difference time domain (FDTD) method is applied in our calculations. The permittivity of gold in the infrared regime is based on the Drude model, $\varepsilon(\omega) = 1 - \omega_p^2/(\omega^2 + i\omega_\tau\omega)$, where $\boldsymbol{\omega}_p$ is the plasma frequency and ω_τ is the damping constant. For gold, the characteristic frequencies are taken as $\omega_p = 1.37 \times 10^{16}$ s^{-1} and $\omega_\tau = 1.2 \times 10^{14}$ s^{-1}.[26,27] The permittivities of the glass substrate and the U-shaped polymer interior structure are taken as 2.00 and 2.25, respectively.[28]

The simulated S parameters are employed to calculate the optical parameters. The reflection is achieved from $R = |S_{11}|^2$, the transmission is achieved from $T = |S_{21}|^2$, and the absorbance is defined as $A = 1–R–T = 1–|S_{11}|^2–|S_{21}|^2$.[10] Figure 1(b) shows the T_x, R_x, and A_x for the x-polarized incidence. In Fig. 1(b), the reflection shows clear resonance at 1170 cm^{-1} where the transmission is almost zero (less than 3‰). The absorbance reaches 96% at 1170 cm^{-1}. For y-polarized incidence, reflection is calculated, and the results are shown in Fig. 1(b). The reflection is higher than 96% and no resonance is detected. In this scenario the SUSR array functions as a reflective mirror. The absorbance calculated at different structural parameters, the height of the horizontal bar

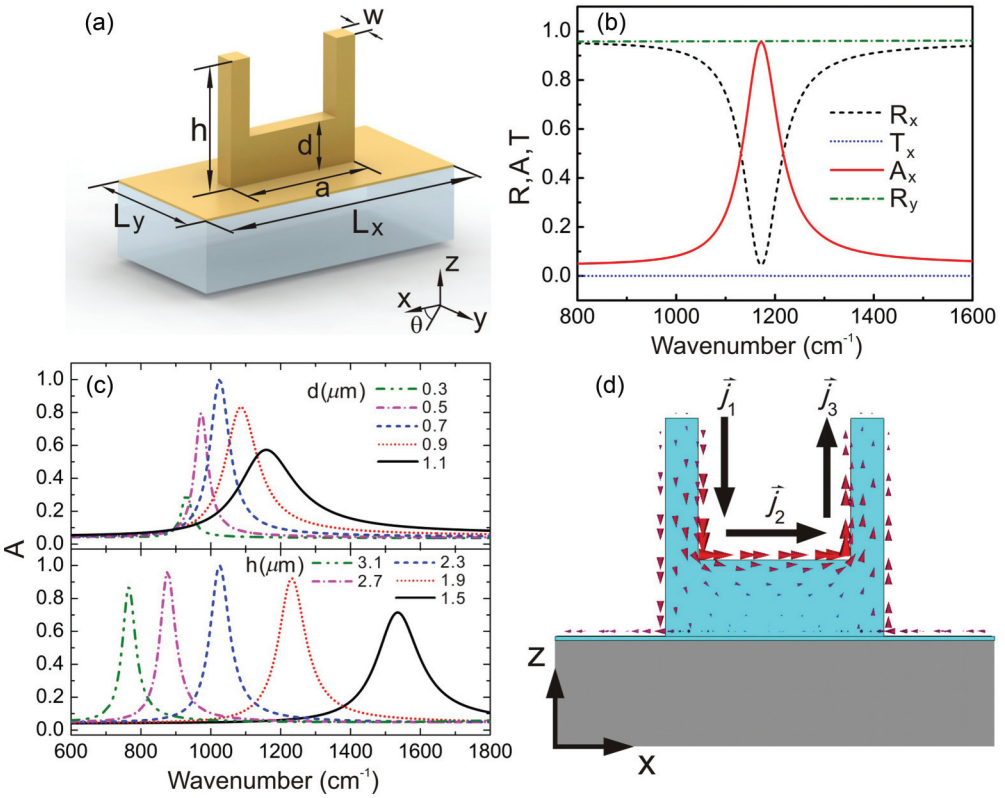

FIG. 1. (Color online) (a) The topography of the SUSR unit: $L_x = 4.0\ \mu$m, $L_y = 2.0\ \mu$m, $a = 2.0\ \mu$m, $h = 2.0\ \mu$m, $d = 0.7\ \mu$m, and $w = 0.3\ \mu$m. (b) The calculated transmission, reflection and absorbance for SUSRs with height $h = 2.0\ \mu$m. (c) The absorbance spectra calculated for different horizontal bar heights ($d = 0.3$, 0.5, 0.7, 0.9, and 1.1 μm, respectively) and for different tine heights ($h = 1.5$, 1.9, 2.3, 2.7, and 3.1 μm, respectively). (d) The simulated distribution of the induced surface electric current at the absorption frequency. Three electric current elements, $\vec{j}_1$, $\vec{j}_2$, and $\vec{j}_3$, are schematically plotted.

(d), and the height of the tine (h) are plotted in Fig. 1(c). By shrinking the height of the horizontal bars, the absorption frequency shifts to the lower frequency. The absorption peak is blueshifted when the height of the horizontal bar of the SUSRs is increased. By shrinking the tine height of the SUSR, the absorption frequency blueshifts; the absorption frequency redshifts when the tine height of the SUSR is increased. Figure 1(c) indicates that the height of the horizontal bar and the height of the tines are efficient parameters to tune the absorption frequency of the SUSRs. One may find that the highest absorbance, 99.6%, can be achieved in the simulation when d is set as 0.7 μm and h is set as 2.3 μm.

III. THEORETICAL CONSIDERATIONS

At the absorption frequency, resonant surface electric current can be excited on the SUSRs by the incident light.[29–32] For a three-dimensional SUSR structure, the electric component of the incident light can excite both the electric and the magnetic responses. The magnetic component of the incident light, at the same time, can also excite both the electric and the magnetic responses. As illustrated in Fig. 1(d), upon illumination of incident light, oscillating electric current can be induced. The induced electric current on the two tines and the horizontal bar can be schematically illustrated by three electric current elements, $\vec{j}_1$, $\vec{j}_2$, and $\vec{j}_3$. These current elements can be viewed as the electric dipoles on the two tines and on the horizontal bar of the structure, and the sum of these electric dipoles does not vanish. Therefore a pure electric dipole exists. On the other hand, $\vec{j}_1$, $\vec{j}_2$, and $\vec{j}_3$ form an open circle, which consequently generates a magnetic dipole. Although it is difficult to calculate the radiation of the structure analytically, the response of the SUSR can be qualitatively analyzed by inspecting the radiation of the surface electric current. The vector potential $\vec{A}$ generated by the structure at the position $\vec{x}$ is expressed by the surface electric current as[33]

$$\vec{A}(\vec{x}) = \frac{\mu_0}{4\pi} \int \vec{j}(\vec{x}') \frac{e^{ik|\vec{x}-\vec{x}'|}}{|\vec{x}-\vec{x}'|} d^3x', \tag{1}$$

where k is the wave number and $\vec{j}(\vec{x}')$ represents the distribution of electric current on the structure. It follows that the radiation fields of the structure can be derived from

$$\vec{H} = \frac{1}{\mu_0} \nabla \times \vec{A}, \quad \vec{E} = \frac{iZ_0}{k} \nabla \times \vec{H}, \tag{2}$$

where $Z_0 = \sqrt{\frac{\mu_0}{\varepsilon_0}}$ is the impedance of free space. In the far field, $|\vec{x} - \vec{x}'| = r - \vec{n} \cdot \vec{x}'$ where $\vec{n}$ is the unit vector in the direction of $\vec{x}$, and r is the amplitude of $\vec{x}$. So Eq. (2) can be simplified as

$$\vec{H} = \frac{1}{\mu_0} \vec{n} \times \frac{\partial \vec{A}}{\partial r}, \quad \vec{E} = \frac{iZ_0}{k} \nabla \times \vec{H}. \tag{3}$$

As the electric current $\vec{j}_1$ and $\vec{j}_3$ are in the z direction, the vector potential $\vec{A}$ generated by these two electric elements is in the z direction as well. According to Eq. (3), $\vec{j}_1$ and $\vec{j}_3$ do not contribute to the radiation in the z direction. Therefore, the radiation of SUSRs in the z direction is contributed mostly by the electric current on the top surface of the horizontal bar, $\vec{j}_2$, which keeps a distance d to the substrate. The oscillating electric current radiates an electromagnetic wave in both the $+z$ and $-z$ directions. Since a homogeneous gold layer has been deposited on the substrate, both the incident light and the radiated light in the $-z$ direction are reflected back by this gold layer. The total reflected light is contributed by the interference of the irradiated light to the $+z$ direction and the light reflected by the homogeneous gold layer. When the phase of the irradiated light is opposite to that of the reflected light, the total reflection is minimized. Therefore, the distance d plays an important role in improving the absorption efficiency of the structure.

The resonance of SUSR can be equivalently treated as a LC circuit and the resonance frequency can be expressed as $\frac{1}{\sqrt{LC}}$. The detailed morphology of the U-shaped resonator determines the value of the effective parameters. Although the surface current on the two standing tines does not contribute to the radiation of SUSR in the z direction, the height of the tines affects the absorption frequency. For this reason, we focus on how the parameters d and h influence the absorption of the structure experimentally in this paper.

IV. EXPERIMENTAL RESULTS AND DISCUSSIONS

To verify the theoretical and numerical results, we fabricate SUSR arrays with a two-photon polymerization system (Nanoscribe GmbH) on a glass plate 170 μm in thickness. The lithography system focuses a femtosecond laser beam to a diffraction-limited spot. The array of SUSRs is fabricated by scanning the focus point in 3D space. The exposed negative photoresist (IP-L, Nanoscribe GmbH) is polymerized and forms the backbone of the standing U-shaped patterns, whereas the unexposed photoresist is removed in the developing process. Thereafter the U-shaped polymer structures are coated with a gold layer 35 nm in thickness by magnetron sputtering to form SUSRs.

Three sets of SUSR arrays are fabricated with different heights of the horizontal bar, d, whereas the height of the tines stays at $h = 2.1$ μm. Figure 2 illustrates the field emission scanning electron micrographs (FESEMs) of the SUSR array with, $d = 0.3$ μm (a), $d = 0.6$ μm (c), and $d = 0.9$ μm (e), respectively. A focal plane array (FPA) microscope (Bruker Hyperion 3000) associated with the Fourier transform infrared (FTIR) spectrometer (Bruker Vertex 70v) is applied to characterize the optical property of SUSRs. A polarizer made of ZnSe is used to tune the polarization of the incident light. In Fig. 2(b) the incident light is x polarized, and d is 0.3 μm. Meanwhile the reflection is 42% and the absorbance reaches 58% at 1060 cm^{-1}. In Fig. 2(d), the absorbance of

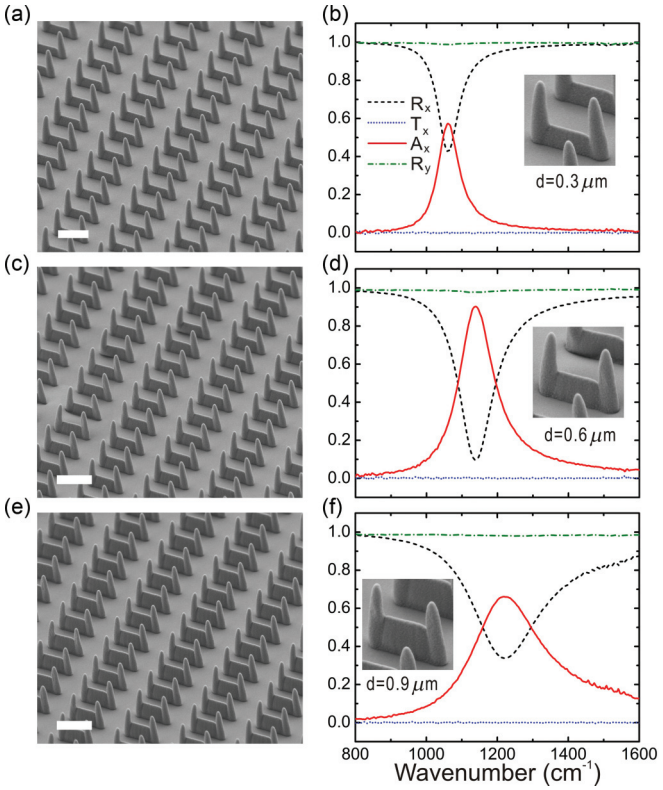

FIG. 2. (Color online) The FESEM micrographs of the SUSRs with different heights of horizontal bar, d. (a) $d = 0.3$ μm, (c) $d = 0.6$ μm, and (e) $d = 0.9$ μm. (b), (d), and (f) show the measured transmission, reflection, and absorbance corresponding to the SUSR array shown in (a), (c), and (e), respectively. The bars in the micrographs represent 2.0 μm.

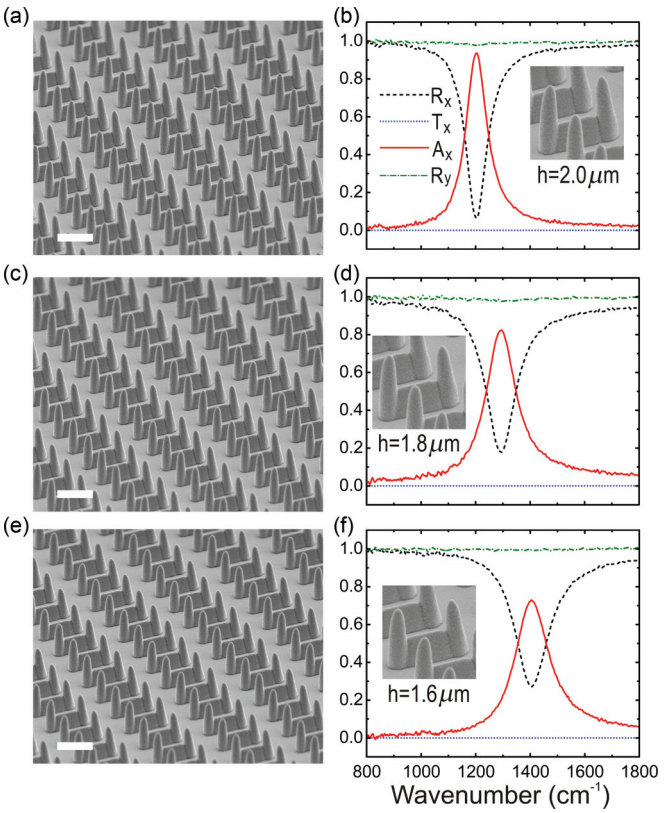

FIG. 3. (Color online) (a), (c), and (e) show the FESEM micrographs of the SUSRs with $h = 2.0$, 1.8 and 1.6 μm, respectively. (b), (d), and (f) show the measured transmission, reflection, and absorbance of the SUSR array shown in (a), (c), and (e), respectively. The bars in the micrographs represent 2.0 μm.

91% is realized at 1135 cm^{-1} for $d = 0.6$ μm. In Fig. 2(f) the absorbance drops to 66% at 1210 cm^{-1} for $d = 0.9$ μm. For all the measurements in Figs. 2(b), 2(d), and 2(f), the transmission is always less than 1%, indicating that light cannot penetrate through the sample. In Figs. 2(b), 2(d), and 2(f) the reflection for y-polarized incidence is also measured. The reflection is larger than 97% for the range between 800 and 1600 cm^{-1} in each measurement; i.e., the SUSR array functions as a reflection mirror. The experiments confirm that d is an important parameter to control the absorption in SUSRs.

We also fabricated three sets of SUSR array with different tine height h; meanwhile the height of the horizontal bar is fixed as $d = 0.7$ μm. The FESEM micrographs of the SUSR array with $h = 2.0$ μm, 1.8 μm, and 1.6 μm, are shown in Figs. 3(a), 3(c), and 3(e), respectively. In Fig. 3(b) the incident light is x polarized, and the tine height is $h = 2.0$ μm. The reflection is less than 7% and the absorbance reaches 94% at 1200 cm^{-1}. In Fig. 3(d), the absorbance of 83% occurs at 1300 cm^{-1} and in Fig. 3(f) the absorbance of 74% is reached at 1400 cm^{-1}. In Figs. 3(b), 3(d), and 3(f), the transmission is always less than 1%. Similarly, for y-polarized incidence, the measured reflection is larger than 97% in the wave band from 800 to 1800 cm^{-1} in each measurement. The experiments confirm that the tine height h is another important parameter to realize perfect absorption.

To demonstrate further the absorption effect of the SUSRs, we fabricate three SUSR arrays with different tine height h side by side on the same glass substrate. The size of each array is 200 μm $\times$ 200 μm. As illustrated in Fig. 4(a), the tine height of the SUSRs in each array, from left to right, is $h = 1.6$, 1.8,

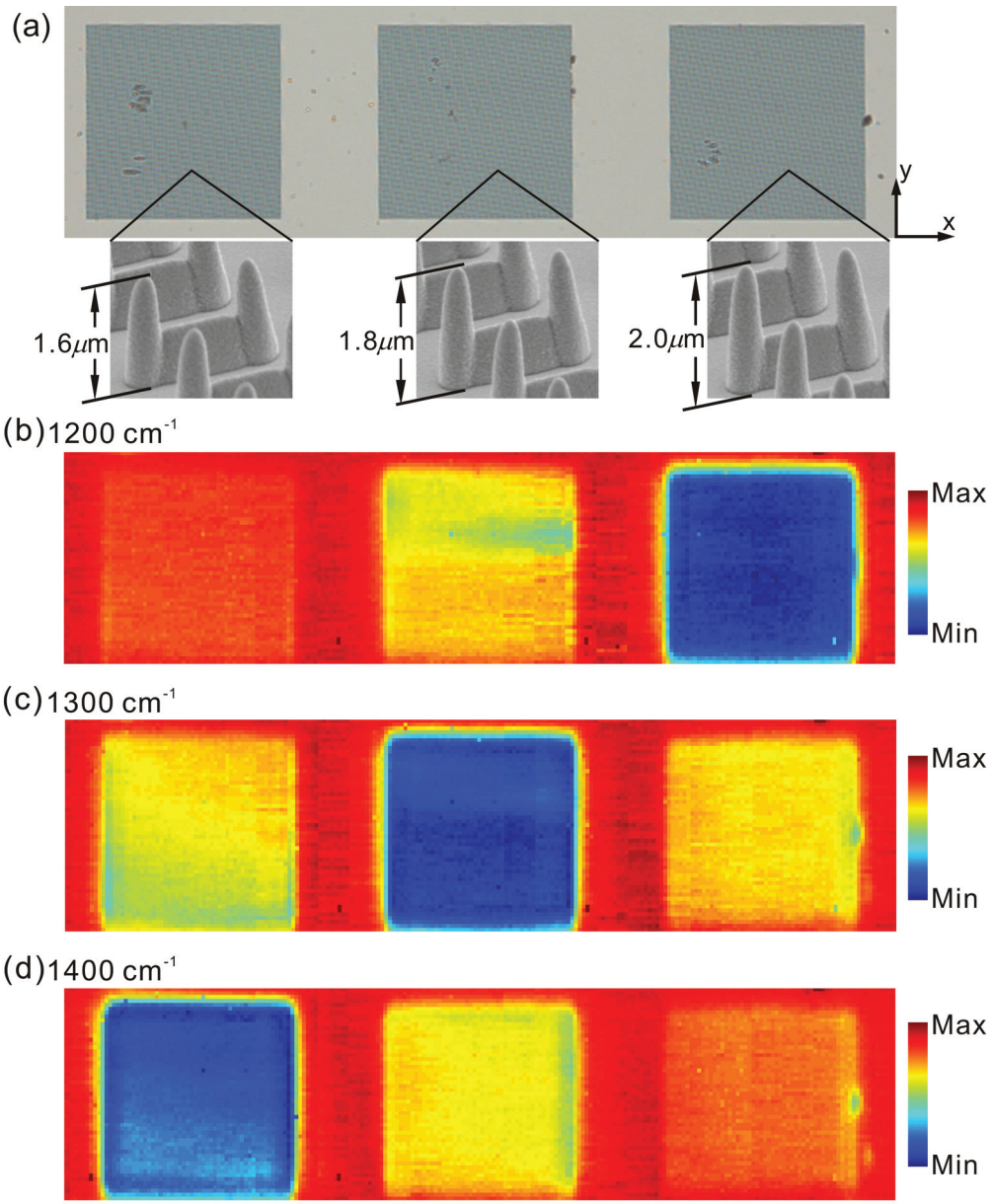

FIG. 4. (Color online) (a) The optical micrograph of SUSR arrays with different tine heights h. The insets show the FESEM micrographs of the SUSR unit in each array, respectively. The FPA images of that shown in (a) have been collected at different wave numbers with x-polarized incidence: (b) 1200 cm^{-1}, (c) 1300 cm^{-1}, and (d) 1400 cm^{-1}.

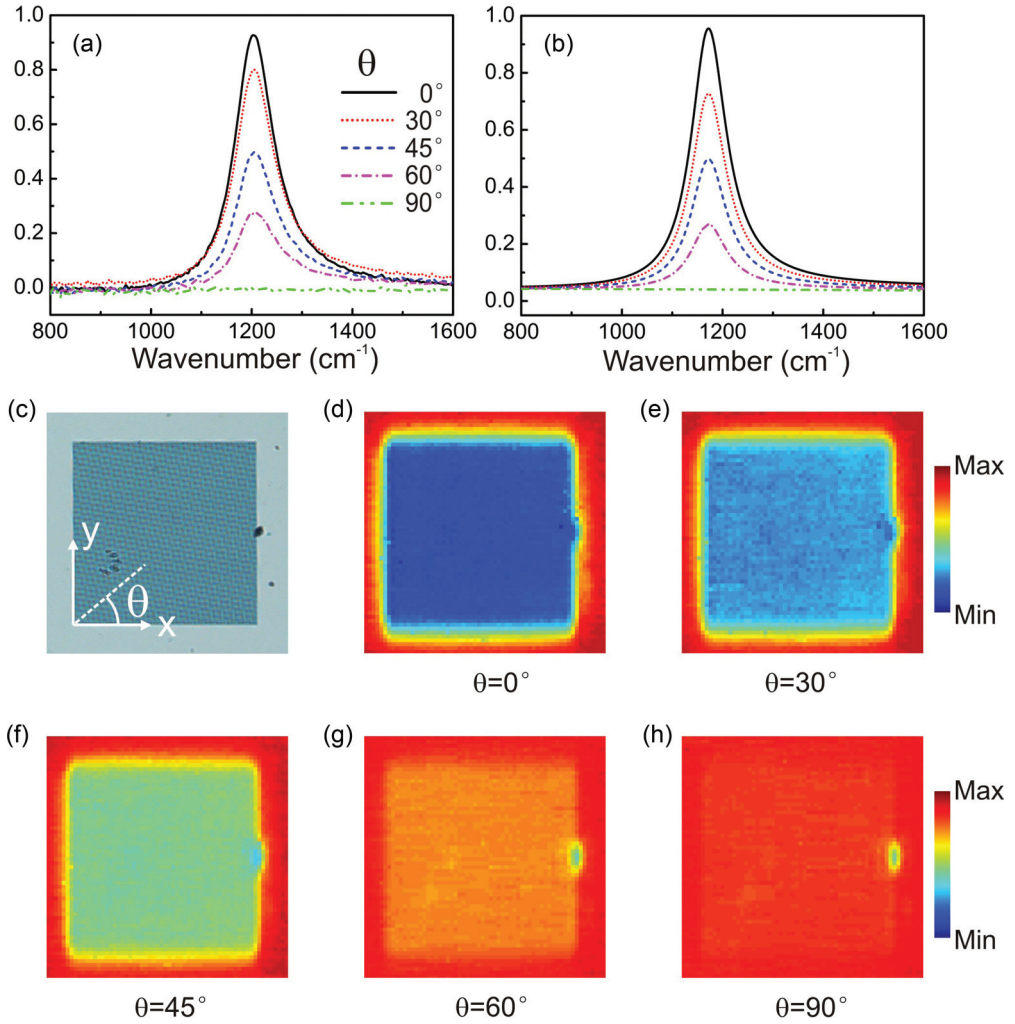

FIG. 5. (Color online) (a) The measured and (b) simulated absorbance of the SUSRs ($h = 2.0$ μm) for different polarized incidence. (c) The micrograph of the SUSRs array to be measured by FPA. The FPA images (d)–(h) are collected at 1200 cm^{-1} for polarization angle $\theta = 0°$, 30°, 45°, 60°, and 90°, respectively.

and 2.0 μm, respectively. The insets in Fig. 4(a) illustrate the detailed morphology of a SUSR unit. The infrared microscope with focal plane array (FPA) detector system (Hyperion 3000, Bruker) collects the infrared signal from the sample. The FPA image is collected at the central wave number with integration width as 20 cm^{-1}. The bright color indicates that more energy is reflected and the absorption is weak; the dark color indicates that most energy has been absorbed and the reflection is weak. The FPA imaging of Fig. 4(b) is collected at 1200 cm^{-1}. The SUSR array with $h = 2.0$ μm shows the strongest absorption effect, whereas the SUSRs with $h = 1.8$ μm and $h = 1.6$ μm show the weaker and weakest absorption, respectively. At 1300 cm^{-1}, the middle array ($h = 1.8$ μm) becomes the darkest, indicating the strongest absorption over the sample. At 1400 cm^{-1}, the leftmost square (with $h = 1.6$ μm) shows the strongest absorption.

For the SUSR array, when the perfect absorption is realized for x-polarized incidence ($\theta = 0°$), perfect reflection occurs simultaneously for y-polarized incidence ($\theta = 90°$). In other words, the SUSRs can act as perfect absorbers or perfect reflectors by merely switching the polarization of the incident light for 90°. To demonstrate this effect experimentally, we select the SUSR array with tine height 2.0 μm. With a ZnSe polarizer, the angle of polarization of the incident light is selected as 0°, 30°, 45°, 60°, and 90°, respectively. The measured data of absorbance are shown in Fig. 5(a), where 94% absorbance is realized for x polarization (polarization angle 0°) at 1200 cm^{-1}. Yet the absorbance is decreased to 80%, 50%, and 28% at the same frequency when the polarization angle changes to 30°, 45°, and 60°, respectively. When the polarization angle reaches 90° (the incident light becomes y polarized), the absorbance decreases to zero. Numerical simulations of FDTD shown in Fig. 5(b) are in excellent agreement with the experiments. Figure 5(c) shows the optical micrograph of the array. FPA measurements are carried out to compare the reflections when the polarization of incident light is changed. Figures 5(d)–5(h) show the FPA images taken at $\theta = 0°$, 30°, 45°, 60°, and 90°, respectively. For $\theta = 0°$, the SUSRs in Fig. 5(d) are dark blue, indicating that very strong absorption has occurred on the sample, and very little energy is collected by the FPA detector. When θ is increased to 30°, 45°, and 60°, the FPA images of

SUSRs become more and more bright, indicating that more and more energy is collected by the detector, and the SUSR array becomes less absorbent. When θ becomes 90°, as shown in Fig. 5(h), it becomes difficult to identify the reflection from the SUSR array and that from the surrounding flat gold surface, indicating that the SUSRs have already become a reflector. Figure 5 suggests that if the unpolarized light (such as natural light) illuminates the SUSR array, the reflected light would be polarized and the polarization direction is along $\theta = 90°$. The component of light with polarization $\theta = 0°$ would have been absorbed.

The energy absorbed by the resonator is mostly transferred to thermal energy.[24] To investigate the thermal stability of our structure, we heat the SUSR sample at different temperatures for a certain period of time by a hot plate in open air and then measure the absorption property. Figure 6(a) shows the FESEM picture of the SUSR array before heating. The transmission, reflection, and absorption in Fig. 6(b) show that 93% absorbance is realized at 1140 cm^{-1}. Then the SUSR sample is placed on the hot plate at 100 °C for 10 min. The SEM topography of the structure after heating is shown in Fig. 6(c) and the corresponding FTIR measurement is shown in Fig. 6(d). One may find that the appearance and optical property of the SUSR array remain unchanged (93% absorbance at 1140 cm^{-1}). The SUSR sample is then heated at 200 °C for 10 min, with the topography and optical properties shown in Figs. 6(e) and 6(f). In Fig. 6(e), the tines of the SUSR become slightly shorter and broader than those shown in Figs. 6(a) and 6(c). At 200 °C the photoresist inside of the gold film becomes softened, and it starts to collapse. FTIR measurement in Fig. 6(f) shows that the absorption frequency is slightly blueshifted for about 10 cm^{-1}, yet the absorbance still reaches 92%. SUSR sample is further heated at 300 °C for 10 min. In Fig. 6(g), it can be seen that the standing tines of the SUSRs begin to tilt. The absorption frequency moves to 1220 cm^{-1}, yet the absorbance remains at 88% despite the deformation of the shape. Finally, the SUSR sample is heated at 350 °C for 10 min. Meanwhile the standing SUSR structures are damaged [Fig. 6(i)] and the array does not exist. FTIR measurement [Fig. 6(j)] suggests that the structure cannot function as an absorber anymore. Figure 6 demonstrates that the negative photoresist we used in the experiment is not strong enough to support the 3D structure at high temperature. We expect that a polymer with a higher softening point and a thicker and stronger coating metal layer would increase the limit of operation temperature further.

Theoretically the absorbance of our structure may reach 99.6%, as shown in Fig. 1(c). In our experiment, however, the fabrication errors in making the 3D structure limit the performance of the absorbers. In the two-photon polymerization process, the tines of the SUSR are fabricated by scanning; i.e., the tines are not fabricated simultaneously. For this reason, the height of the neighboring tines can be slightly different. In addition, the surface tension in the developing and drying process tends to attract the neighboring tines. These defects become even more evident when the tines of the SUSRs become higher. These restrictions limit the maximization of the absorbance of the experimentally fabricated 3D structure. Moreover, the finite size and ellipsoidal shape of the focus point in a two-photon polymerization system also restrict

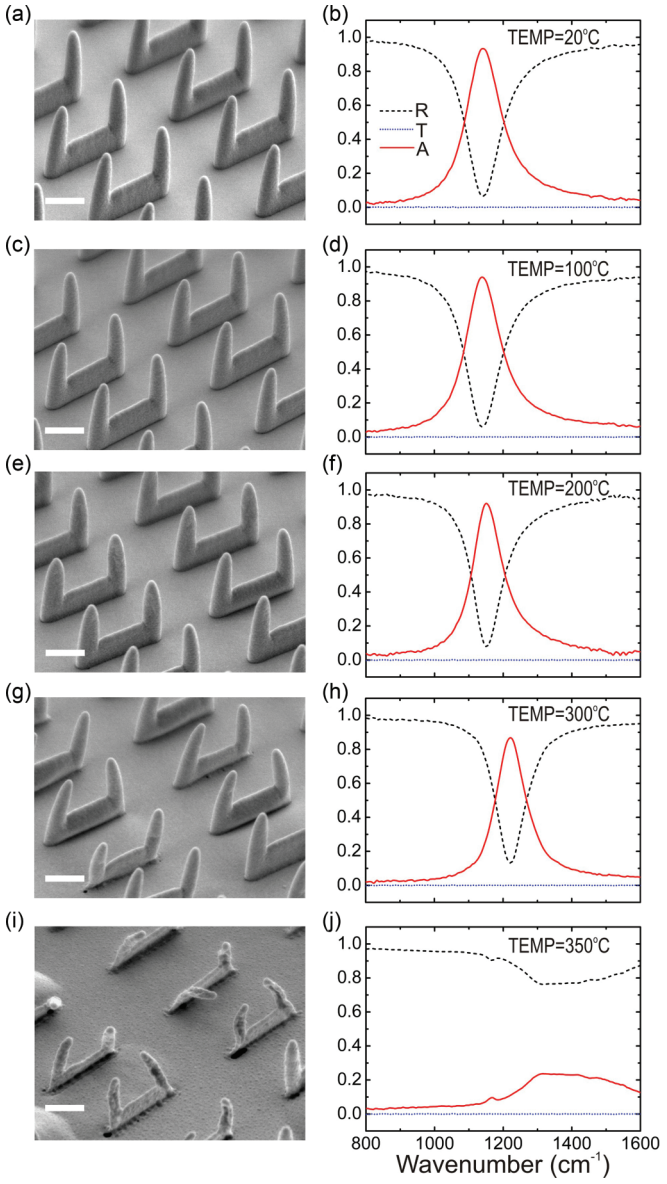

FIG. 6. (Color online) (a), (c), (e), (g), and (i) show the FESEM micrographs of the SUSRs heated at the temperature 20 °C, 100 °C, 200 °C, 300 °C, and 350 °C, for 10 min, respectively. (b), (d), (f), (h), and (j) illustrate the corresponding measured transmission, reflection, and absorbance of the SUSR array. The bars in the micrographs represent 1.0 μm.

the morphology of the fabricated structure. For example, in fabricating the tines of SUSRs, the focus point is moved in a vertical line. For this reason, the cross section of the tine is in a circular shape instead of a square in the design [Fig. 1(a)]. Besides, the tip of the tine is cone shaped, since the focus point of the laser beam is ellipsoidal. The slightly larger cross-section size of the tine near the bottom of the structure is due to the slower moving speed of the laser focus point in fabrication, with the purpose to enhance the mechanical stability of the structure. Numerical simulation indicates that the resonant frequency for SUSRs with cone-structured tines has been increased with respect to that of the square-columned tines. For example, the absorption frequency is 1270 cm^{-1} for

cone-structured tines with bottom radius as 200 nm instead of 1170 cm^{-1} for the square-columned tines in calculation [Figs. 1(a) and 1(b)]. On the other hand, the cone shape itself also affects the resonant frequency. We change the slope of the cone-structured tine by keeping the tine height as a constant (2.0 μm in our case), and increasing the bottom radius of the cone. It turns out that when the bottom radius is increased from 200 to 500 nm, the absorption wave number shifts from 1270 to 1400 cm^{-1} corresponding to the absorption better than 95%. Therefore the resonance frequency is closely related to the detailed morphology of SUSRs.

V. CONCLUSIONS

We report in this paper an approach to fabricate 3D polarization-sensitive metamaterial absorption with SUSRs. For a selected polarization, the SUSRs can act as a perfect absorber, and the incident light may neither transmit nor reflect from the surface. When the polarization of incident light has been rotated for 90°, the incident light reflects perfectly and the SUSR structure functions as a mirror. Experimental data are in good agreement with the calculations. We also find that the absorption of the structure is sensitive to the polarization of the incident light. For this reason, SUSRs may act as polarization detectors as well. Thermal stability of the absorbance of the SUSR array has been studied. With our current structural parameters, the SUSR absorber may work up to 300 °C for 10 min.

ACKNOWLEDGMENTS

This work has been supported by the grants from the State Key Program for Basic Research from MOST of China (Grants No. 2010CB630705 and No. 2012CB921502), the NSF of China (Grants No. 11204127, No. 11034005, and No. 61077023), the MOE of China (SRFDP No. 20120091120033), and partly by Jiangsu Province (Grant No. BK 2012301).

*muwang@nju.edu.cn

[1] J. M. Enoch, Optom. Vision Sci. **83**, 775 (2006).
[2] H. A. Macleod, *Thin-film Optical Filters*, 2nd ed. (Macmillan, New York, 1986).
[3] Y. Wang, T. Sun, T. Paudel, Y. Zhang, Z. Ren, and K. Kempa, Nano Lett. **12**, 440 (2012).
[4] T. Maier and H. Brueckl, Opt. Lett. **34**, 3012 (2009).
[5] X. L. Liu, T. Starr, A. F. Starr, and W. J. Padilla, Phys. Rev. Lett. **104**, 207403 (2010).
[6] F. Ghmari, T. Ghbara, M. Laroche, R. Carminati, and J. J. Greffet, J. Appl. Phys. **96**, 2656 (2004).
[7] N. Liu, M. Mesch, T. Weiss, M. Hentschel, and H. Giessen, Nano Lett. **10**, 2342 (2010).
[8] D. Shrekenhamer, W. R. Xu, S. Venkatesh, D. Schurig, S. Sonkusale, and W. J. Padilla, Phys. Rev. Lett. **109**, 177401 (2012).
[9] L. Meng, D. Zhao, Q. Li, and M. Qiu, Opt. Express **21**, A111 (2013).
[10] N. I. Landy, S. Sajuyigbe, J. J. Mock, D. R. Smith, and W. J. Padilla, Phys. Rev. Lett. **100**, 207402 (2008).
[11] H. Li, L. H. Yuan, B. Zhou, X. P. Shen, Q. Cheng, and T. J. Cui, J. Appl. Phys. **110**, 014909 (2011).
[12] L. Huang, D. R. Chowdhury, S. Ramani, M. T. Reiten, S. N. Luo, A. J. Taylor, and H. T. Chen, Opt. Lett. **37**, 154 (2012).
[13] D. Y. Shchegolkov, A. K. Azad, J. F. O'Hara, and E. I. Simakov, Phys. Rev. B **82**, 205117 (2010).
[14] H. Tao, C. M. Bingham, D. Pilon, K. B. Fan, A. C. Strikwerda, D. Shrekenhamer, W. J. Padilla, X. Zhang, and R. D. Averitt, J. Phys. D **43**, 225102 (2010).
[15] H. Y. Zheng, X. R. Jin, J. W. Park, Y. H. Lu, J. Y. Rhee, W. H. Jang, H. Cheong, and Y. P. Lee, Opt. Express **20**, 24002 (2012).
[16] K. Chen, R. Adato, and H. Altug, ACS Nano **6**, 7998 (2012).
[17] Y. X. Cui, K. H. Fung, J. Xu, H. J. Ma, Y. Jin, S. L. He, and N. X. Fang, Nano Lett. **12**, 1443 (2012).
[18] F. Ding, Y. X. Cui, X. C. Ge, Y. Jin, and S. L. He, Appl. Phys. Lett. **100**, 103506 (2012).
[19] Q. Y. Wen, H. W. Zhang, Y. S. Xie, Q. H. Yang, and Y. L. Liu, Appl. Phys. Lett. **95**, 241111 (2009).
[20] K. Aydin, V. E. Ferry, R. M. Briggs, and H. A. Atwater, Nat. Commun. **2**, 517 (2011).
[21] Y. Ma, Q. Chen, J. Grant, S. C. Saha, A. Khalid, and D. R. S. Cumming, Opt. Lett. **36**, 945 (2011).
[22] C. H. Wu, B. Neuner, G. Shvets, J. John, A. Milder, B. Zollars, and S. Savoy, Phys. Rev. B **84**, 075102 (2011).
[23] W. C. Chen, M. Koirala, X. L. Liu, T. Tyler, K. G. West, C. M. Bingham, T. Starr, A. F. Starr, N. M. Jokerst, and W. J. Padilla, arXiv:1212.2868.
[24] X. Chen, Y. T. Chen, M. Yan, and M. Qiu, ACS Nano **6**, 2550 (2012).
[25] J. Wang, Y. T. Chen, X. Chen, J. M. Hao, M. Yan, and M. Qiu, Opt. Express **19**, 14726 (2011).
[26] N. Liu, L. Langguth, T. Weiss, J. Kastel, M. Fleischhauer, T. Pfau, and H. Giessen, Nat. Mater. **8**, 758 (2009).
[27] G. Dolling, C. Enkrich, M. Wegener, C. M. Soukoulis, and S. Linden, Science **312**, 892 (2006).
[28] M. Schroeder, M. Buelters, C. von Kopylow, and R. B. Bergmann, J. Eur. Opt. Soc, Rapid Publ. **7**, 12027 (2012).
[29] J. B. Pendry, A. J. Holden, D. J. Robbins, and W. J. Stewart, IEEE Trans. Microwave Theory Tech. **47**, 2075 (1999).
[30] X. Xiong, W. H. Sun, Y. J. Bao, R. W. Peng, M. Wang, C. Sun, X. Lu, J. Shao, Z. F. Li, and N. B. Ming, Phys. Rev. B **80**, 201105(R) (2009).
[31] X. Xiong, W. H. Sun, Y. J. Bao, M. Wang, R. W. Peng, C. Sun, X. Lu, J. Shao, Z. F. Li, and N. B. Ming, Phys. Rev. B **81**, 075119 (2010).
[32] K. B. Fan, A. C. Strikwerda, H. Tao, X. Zhang, and R. D. Averitt, Opt. Express **19**, 12619 (2011).
[33] J. D. Jackson, *Classical Electrodynamics*, 3rd ed. (Wiley, New York, 1999).